This article is the accepted version of *A. Yonezawa, H. Yonezawa, I. Kajiwara, "Efficient parameter tuning to enhance practicability of a model-free vibration controller based on a virtual controlled object," Mechanical Systems and Signal Processing, 200 (2023) 110526.* (https://doi.org/10.1016/j.ymssp.2023.110526)

Efficient parameter tuning to enhance practicability of a model-free vibration controller based on a virtual controlled object

Ansei Yonezawa, Heisei Yonezawa, Itsuro Kajiwara*

Division of Mechanical and Aerospace Engineering, Hokkaido University

N13, W8, Kita-ku, Sapporo 060-8628, Japan

* Corresponding author

E-mail: ikajiwara@eng.hokudai.ac.jp

Abstract

In active vibration control, controller tuning is necessary to obtain a sufficient damping performance. This study presents an efficient tuning technique for model-free vibration controller based on a virtual controlled object (VCO). A model-free vibration control system is constructed by using an actuator model and the VCO. A reference controlled object (RCO), which is a designer-defined single-degree-of-freedom (SDOF) structure, is used to tune the VCO-controller offline. A novel parameter tuning technique based on the RCO and the simultaneous perturbation stochastic approximation (SPSA) is proposed considering the difference in scale of the tuning parameters. The proposed tuning scheme automatically determines the tuning parameter of the controller without manual trial-and-errors such as experiments with actual plants and is much faster than previous methods. Therefore, the proposed method significantly enhances the practicability of the VCO-based model-free vibration suppression, bridging the gap between the basic study of the VCO-method and its implementation. The effectiveness of the proposed method is verified by applying it to the VCO-based H_2 controller.

Keywords

Active vibration control, Model-free control, Virtual controlled object, Simultaneous perturbation stochastic approximation, Optimization, H_2 control.

1. Introduction

1.1. Motivation

Vibration reduction technology is indispensable for improving performance and safety of mechanical systems. Various vibration suppression strategies have been examined for challenging vibration problems: bio-inspired nonlinear dynamics [1–4], origami-based vibration isolator [5,6], and mode-switching scheme [7–9], to name a few. Among them, active vibration control is widely developed because of its good vibration reduction performance [10,11]. For example, disturbance rejection methods have been proposed for a magnetic-head positioning system in hard disk drives [12–14]; sliding mode control has been applied for a building structure [15] and a milling system [16]; active vibration control for planetary gearbox have been proposed [17]. In general, controllers are designed using concrete mathematical models of controlled objects (e.g., [18,19]). However, modeling of controlled object is burdensome and costly. Control system construction without modeling actual controlled objects in detail, model-free control, can reduce the development cost and burden.

1.2. Related work: Model-free control

Many researchers have attempted to construct various control systems without using concrete models of actual controlled objects [20,21]. For example, the tube-based model-reference adaptive vibration control has been examined for active car suspension system [22]. Controller design via artificial intelligence (e.g., neural networks) is a powerful method to derive model-free controllers [23–25]. In particular, the radial basis function neural network (RBFNN) has been employed in a Nussbaum gain adaptive control to identify unknown plant nonlinearities [26]; parametric variations and unmodeled dynamics in multiple launch rocket system has been estimated via the RBFNN [27]. However, this technique typically requires a huge amount of training data, increasing the associated development costs. The fuzzy control approach is an effective method to construct model-free control systems [28–30]. Nevertheless, fuzzy control often relies on the experience and intuition of the designers because there are no systematic approaches to determine control rules. Data-driven controller design is a typical model-free control approach [31,32]. However, data-driven control methods are fragile to changes in characteristics of controlled objects. Active disturbance rejection control (ADRC) [33] is also a good control method which does not need exact plant models. The key idea of ADRC is innovative: unknown dynamics of a plant and external disturbances are lumped into a "total disturbance," estimated by an extended state observer (ESO) and canceled out. Many studies have examined to implement ADRC into various mechanical systems [34–36]. The formulation of the lumped disturbance, however, is not always straightforward depending on systems, complicating the design process of ADRC. Table 1 lists typical ways to develop a control system without detailed modeling of an actual controlled object, indicating that the existing model-free control approaches have several difficulties which deteriorate the practicability.

By contrast, model-free active vibration control based on a virtual controlled object (VCO) has a simpler controller design process and is easier to implement than existing model-free control approaches [37,38]. In this approach, only the VCO, which is a single-degree-of-freedom (SDOF) structure, and the actuator model are required to design a vibration controller.

The appropriate VCO to realize model-free control can be easily designed based on the quantitative design condition discussed in the previous study, and the controller can be systematically designed by directly using familiar model-based control theories (e.g., the linear quadratic regulator (LQR) theory) after the introduction of the VCO [37]. It should be noted that the VCO-based model-free controller has some tuning parameters that can be adjusted [39–41]. Therefore, a simple, quantitative, and practical parameter tuning strategy is needed to enhance the practicability of the VCO-based model-free vibration control.

Table 1. Typical model-free control strategies.

Strategy	Example	Advantage	Disadvantage
Neural network	Vibration control for flexible cantilever via neurocontroller [23]. Approximation of nonlinear, uncertain, and unknown dynamics [24–27].	Applicable to wide range of plant and dynamics.	Necessity of huge amount of training data
Fuzzy logic	Fuzzy Luenberger observer for a two-mass drive system [28]. Vibration control of uncertain structures with actuator saturation [29]. Fuzzy sliding mode vibration control for flexible structure [30].	Easy to reflect experience and intuition of plants.	Lack of systematic approach to design inference rules
Data-driven control	Fictitious reference iterative tuning (FRIT) [31]. Virtual reference feedback tuning (VRFT) [32].	Systematic controller design procedure.	Fragile to changes in characteristics of plants
ADRC	Structural vibration control for piezoelectric beam [35] Robust active vibration suppression for two-inertia system [34]	Good control performance.	Complicated design process depending on a plant.

1.3. Related work: Controller tuning via optimization approach

Several groups have examined controller tuning based on optimization methods: genetic algorithm [42,43], particle swarm algorithm [44], gravitational search algorithm [45], and grey wolf optimizer [46–48]. Metaheuristic optimization tools are developed for a Gaussian adaptive PID controller [49]. Among them, the simultaneous perturbation stochastic approximation (SPSA) [50] is frequently used to tune a controller [51,52]. The most representative virtue of SPSA is its high calculation efficiency in the sense that SPSA requires very small number of loss function evaluations even for high-dimensional problems.

Inspired by these studies, a parameter tuning scheme for the VCO-based model-free controller has been proposed [53]. In this scheme, the damping performance of the controller is evaluated via vibration control simulations with a reference controlled object (RCO) instead of real plant models and then the VCO-controller is iteratively tuned by SPSA. Therefore, this tuning scheme does not require burdensome manual controller parameter adjustments (e.g., trial-and-error tuning through vibration control experiments with real plants). However, this tuning scheme does not adequately take the characteristic of SPSA into account (e.g., in SPSA, the scales of the design variables should be similar to each other [54]) and is not efficient enough to use on-site. Consequently, faster and more efficient tuning scheme is needed to bridge the gap between the basic study of the VCO-based vibration control and its practical implementation.

1.4. Contribution and novelty of this study

In this study, we propose a novel parameter tuning scheme for the VCO-based model-free controller. The proposed method is more practical in the sense that it is much faster than the previous one [53]. The model-free vibration control system is constructed by inserting the SDOF VCO between the actuator model, which can be modeled as an SDOF system, and the actual controlled object. The model-free controller is designed with a two-degree-of-freedom (2DOF) system composed of the actuator and the VCO. The loss function and the SDOF RCO are defined to evaluate the damping performance of the VCO-based model-free controller to tune its parameters. Notably, the RCO is not an actual controlled object but a designer-defined structure. The controller parameters to be tuned are expressed using a novel parameter scaling rule to overcome their scale difference. Vibration control simulations are conducted with the RCO, and the scaled tuning parameters of the VCO-controller are iteratively determined to minimize the loss function by SPSA. The advantage of the proposed tuning method is that the tuning speed is much faster than that of the previous method for the VCO-controller [53], enhancing the practicability of the VCO-based vibration control. We compare the tuning speed of the proposed technique with that of the previous technique by applying them to the VCO-based model-free H_2 controller tuning problem. Finally, the damping performance of the VCO-based H_2 controller tuned by the proposed method is examined by experiments.

The contribution of this study includes:

1) The novel controller tuning method for the VCO-based model-free vibration control is proposed. This method can tune the VCO-controller much faster and easier than the previous tuning methods, enhancing the practical usability of the VCO-based model-free vibration control. (Note that controller tuning is a central task to implement a control system in practice.) Moreover, unlike the traditional tuning methods for model-based controllers, the proposed method uses the SDOF RCO instead of the actual plant model, reducing the development cost. This advantage originates from the strong robustness of the VCO-based controller to changes in actual controlled objects.

2) The VCO-based model-free H_2 controller is automatically tuned without manual trial-and-errors for the first time. In previous studies, VCO-based model-free controllers were mainly tuned by manual trial-and-errors. The tuning of the VCO-based model-free H_2 controller is a typical application example showing the wide applicability of the proposed tuning scheme.

The VCO-based model-free vibration control can be employed for various vibration problems because this method does not depend on the specific properties of controlled objects

[53]. Accordingly, the proposed tuning method simplifies the implementation process of the VCO-method and provides a simple and practical solutions to various vibration problems in mechanical systems including industrial applications.

2. VCO-based model-free vibration control

This study uses an electromagnetic proof-mass actuator. This actuator can be modeled as an SDOF system because of its mechanical properties [37].

VCO-based model-free vibration control is achieved by inserting the SDOF VCO between the actuator and an actual controlled object [37]. Figure 1(a) shows the actual mechanical system. m_0, k_0, and c_0 represent the mass, stiffness, and damping of the actuator, respectively. x_0 and x_1 are the displacement of the point mass of the actuator and that of the location on the actual controlled object where its vibrations should be attenuated, respectively. Hereafter, this location is called as the damping point. VCO-based model-free vibration control is implemented by directly attaching an actuator and a sensor to the damping point. The aim of this active vibration control system is to attenuate the vibration x_1 of the damping point by the control input force u generated by the actuator. Notably, the concrete characteristics and structures of the actual controlled object are not considered.

Figure 1(b) shows the system for the model-free controller design, where the VCO is introduced between the actuator and the actual controlled object. m_v, k_v, and c_v represent the mass, stiffness, and damping of the VCO, respectively, and x_v is the displacement of the point mass of the VCO. The key idea of the VCO-based model-free vibration control strategy is that the VCO is regarded as the controlled object and x_1 is indirectly damped by damping x_v [37]. The controller is designed using the 2DOF system composed of only the actuator and the VCO.

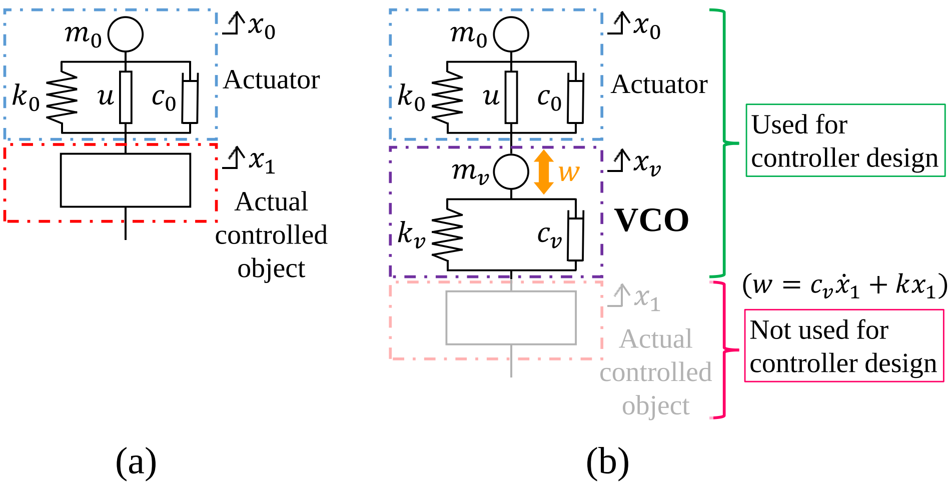

Fig. 1. Vibration control system: (a) actual mechanical system, and (b) system for model-free controller design. An SDOF VCO is inserted between the actuator and the actual controlled object.

m_v and k_v are designed to establish model-free control. Specifically, they are determined so that $x_v \approx x_1$ is realized in the controlled frequency band. A quantitative design condition for m_v and k_v to realize $x_v \approx x_1$ in the controlled frequency band is derived in [37]. Notably, as shown in [37], m_v and k_v to achieve $x_v \approx x_1$ can be specified independently of detailed mathematical models of actual controlled objects. Only the controlled frequency band is required as the information about the actual controlled object to determine them. Table 2 lists the parameter values of the actuator and the VCO used in this study [37]. The controlled frequency band is 50–1000 Hz.

Using the equations of motion of the actuator and the VCO shown in Fig. 1(b), the state equation to design the VCO-based model-free controller is derived as [37]:

$$\dot{x}_{mf} = A_{mf}x_{mf} + B_{mf1}w + B_{mf2}u \tag{1}$$

$$x_{mf} = [x_v \quad x_0 \quad \dot{x}_v \quad \dot{x}_0]^T \tag{2}$$

$$A_{mf} = \begin{bmatrix} 0 & 0 & 1 & 0 \\ 0 & 0 & 0 & 1 \\ -\dfrac{k_0 + k_v}{m_v} & \dfrac{k_0}{m_v} & -\dfrac{c_0 + c_v}{m_v} & \dfrac{c_0}{m_v} \\ \dfrac{k_0}{m_0} & -\dfrac{k_0}{m_0} & \dfrac{c_0}{m_0} & -\dfrac{c_0}{m_0} \end{bmatrix} \tag{3}$$

$$B_{mf1} = \begin{bmatrix} 0 & 0 & \dfrac{1}{m_v} & 0 \end{bmatrix}^T \tag{4}$$

$$B_{mf2} = \begin{bmatrix} 0 & 0 & -\dfrac{1}{m_v} & \dfrac{1}{m_0} \end{bmatrix}^T \tag{5}$$

In Eq. (1), x_{mf} is the state variable of the 2DOF system composed of the velocity and displacement of the point masses of the actuator and the VCO. The force $c_v\dot{x}_1 + k_v x_1$, which is caused by the vibration of the actual controlled object, is regarded as the disturbance w acting on the 2DOF system composed of the actuator and the VCO so that any parameters and variables of the actual controlled object are not included in the state equation for model-free controller design [37].

Equation (1) contains no parameters or models of the actual controlled object. Therefore, model-free vibration suppression is achieved by designing the controller using Eq. (1). The controller based on Eq. (1) indirectly suppresses the vibration of the actual controlled object because $x_v \approx x_1$ is realized. The VCO-based model-free controller is easily obtained by applying familiar model-based control theories to Eq. (1).

Here, the VCO-based model-free vibration control has different idea from ADRC in the control action. In particular, the VCO-method only focuses on stabilizing the VCO under disturbance as traditional model-based feedback controller and does not require an explicit value of the total disturbance, whereas ADRC explicitly estimates it through the ESO and cancels it out directly. One important advantage of the VCO-based control method over ADRC is its simplicity: the controller design of the VCO-method is easier than that of ADRC. In ADRC design, a key point is how to identify the effects of the unknown dynamics and external disturbances and define them as the total disturbance, requiring deep insight into the plant characteristics. In addition, the order of ADRC is determined according to the relative degree of the plant [33,55]. Obtaining the relative degree of the plant is not always straightforward [33], and the relative degree of the plant significantly affects the design complexity [33]. In contrasts, the VCO-method can directly utilize familiar model-based control theories after the introduction of the VCO. The VCO itself can be easily designed according to the design condition proposed in the previous study [37]; this design condition requires only an actuator model and upper and lower bounds of the controlled frequency band, and such information can be obtained easily. Hence, designing the VCO-controller is easy and straightforward.

The VCO-based model-free vibration control is established by feeding the vibration response of the VCO back as the measured output. In the actual feedback control, the vibration of the actual controlled object x_1, which is almost equal to x_v, is used for the measured output instead of x_v because the VCO does not exist in the actual mechanical system. The value of x_1 is measured by a sensor when continuous structures are the actual controlled object [37]. Consequently, both actuator and the sensor for obtaining measured outputs are assumed to be attached at the damping point.

One of the unique characteristics of the VCO-based model-free control is that the VCO-controller has strong robustness to various changes in actual objects [53]. It should be noted that the VCO-controller does not depend on the detailed mathematical models of actual plants although some rough plant information, namely, the controlled frequency band, is used. Specifically, the VCO-controller works relying on only the measured vibration response of the actual controlled object. That is, the VCO-controller suppresses vibrations based on its amplitude regardless of the detailed vibration characteristics such as mode shapes. This independence from the detailed characteristics of the specific controlled object implies that the VCO-based controller can accept various controlled objects as far as vibrations to be suppressed occur within the controlled frequency band. The detailed dynamics of the actual plant do not critically affect the control action of the VCO-controller. Accordingly, the VCO-based model-free controller exhibits strong robustness to various changes in actual objects.

Table 2. Parameters for model-free control system design.

Properties	Value	Unit
m_0	0.2013	kg
k_0	3518	N/m
c_0	1.186	Ns/m
m_v	1.0×10^{-5}	kg
k_v	7.0×10^{5}	N/m
c_v	0.0	Ns/m

3. Efficient controller tuning for VCO-based model-free vibration control

A novel efficient controller tuning based on the RCO and SPSA is proposed for the VCO-based model-free control. In this method, the controller parameters to be tuned are transformed into parameters suitable to optimize by SPSA. Hereafter, the controller parameter to be determined is referred to as a tuning parameter, and the transformed parameter to be updated directly by SPSA during the tuning scheme is referred to as a design variable. Consequently, the parameters of the VCO-controller (i.e., the tuning parameters) are indirectly optimized through the transformed parameters (i.e., the design variables) via SPSA.

3.1. RCO and loss function

This section describes the RCO and the loss function, which are used for the novel tuning scheme for the VCO-based model-free controller proposed in this study. The VCO-controller is robust against characteristic changes and structural changes in actual controlled objects [53]. Focusing on the strong robustness of the VCO-based model-free controller, an automatic controller parameter tuning has been proposed [53]. This procedure determines the appropriate controller parameter through offline vibration control simulations with the RCO instead of the actual controlled objects. Figure 2 describes the RCO, which is a designer-defined SDOF structure. m_r, k_r, and c_r are the mass, stiffness, and damping of the RCO, respectively. The design policy of the RCO has been discussed in a previous study [53]. Especially, the RCO must be designed so that it has the natural frequency in the controlled frequency band of the VCO-controller where $x_v \approx x_1$ holds. That is, the RCO and the actual controlled object share the frequency band where the vibrations to be attenuated by the VCO-controller occur. Notably, the VCO-based controller tuned for the RCO can suppress the vibration of various controlled objects other than the RCO in the controlled frequency band because of the key condition $x_v \approx x_1$ and the robustness of the VCO-controller [53]. In this study, $m_r = 1.2$ kg, $k_r = 1.0 \times 10^6$ N/m, and $c_r = 1.095 \times 10^1$ Ns/m [53].

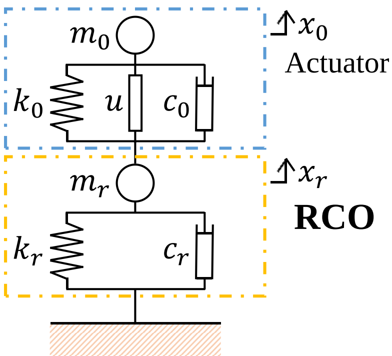

Fig. 2. The RCO.

Note that the parameter tuning based on the RCO does not require detailed mathematical modeling of the actual controlled object. That is, the RCO-based controller parameter tuning can be regarded as a model-free; hence, it is simple and easy to implement. Accordingly, this study employs the RCO.

The damping performance for the RCO provided by the VCO-based model-free controller is evaluated via the loss function. The VCO-controller is tuned to minimize the loss function value in the proposed method. Let $L(\theta) > 0$ be the loss function to be minimized and $\theta \in \mathbb{R}^p$ be the design variable. Index k represents the kth iteration. Equation (6) is the loss function used in this study [53]:

$$L(\theta_k) = \frac{1}{N}\left\{W_y\left(\sum_{n=1}^{N} {y_{k,n}}^2\right) + W_u\left(\sum_{n=1}^{N} {u_{k,n}}^2\right)\right\} \tag{6}$$

where $y_{k,n}$ is the vibration response (measured output) at the nth sampling point, $u_{k,n}$ indicates the control input at the nth sampling point, N represents the number of sampling points in each simulation, and W_y and W_u are weights on $y_{k,n}$ and $u_{k,n}$, respectively. In this study, $W_y = 1$ and $W_u = 30$. W_y and W_u can be adjusted according to the required performance [53]. The proposed tuning method can avoid excessive high-gain controllers due to the second term of the right-hand side of Eq. (6). If the controller has high-gain and generates too much control input, this term becomes very large, resulting in a very large loss function value.

3.2. Loss function minimization via SPSA

The proposed method tunes the VCO-controller to minimize $L(\theta)$ via SPSA. Let $J(\theta)$ be the measurement of $L(\theta)$. That is, $J(\theta_k) = J_k$ represents the measured value of $L(\theta_k)$ obtained from the result of the damping simulation with a closed-loop system composed of the RCO and the VCO-controller based on θ_k. The θ update rule by SPSA to minimize the loss function $L(\theta)$ [50] is

$$\theta_{k+1} = \theta_k - a_k \frac{J(\theta_{k+}) - J(\theta_{k-})}{2c_k} \Delta_k^{(-1)} \tag{7}$$

$$\theta_{k\pm} = \theta_k \pm c_k \Delta_k \tag{8}$$

$$\Delta_k = [\Delta_{k,1} \quad \Delta_{k,2} \quad \cdots \quad \Delta_{k,p}]^T \tag{9}$$

$$\Delta_k^{(-1)} = \left[(\Delta_{k,1})^{-1} \quad (\Delta_{k,2})^{-1} \quad \cdots \quad (\Delta_{k,p})^{-1}\right]^T \tag{10}$$

where $\Delta_k \in \mathbb{R}^p$ is a random perturbation vector satisfying certain conditions (e.g., Bernoulli ± 1 distribution with a probability of 0.5 for each ± 1) [50], and $\Delta_{k,i}$ is the ith element of Δ_k. Equation (11) shows a_k and c_k used in this study where a, A, c, α, and γ are positive constants.

$$a_k = a(A + k)^{-\alpha}, c_k = ck^{-\gamma} \tag{11}$$

One of the most distinctive features of SPSA is its high calculation efficiency. In general, obtaining measurements of a loss function is a burdensome task in optimization [56]. However, SPSA requires only two measurements of the loss function per iteration, irrespective of p. Therefore, this study uses SPSA as a basic optimization strategy.

3.3. Novel scaling technique for controller tuning

To ensure efficient optimization by SPSA, the scales of the parameters to be optimized should be similar to each other [54]. Nevertheless, the tuning parameters of the VCO-based controller often have large scale differences [53]. Here, the tuning parameter at the kth iteration is denoted as $Q_k = [Q_{k,1} \quad Q_{k,2} \quad \cdots \quad Q_{k,j} \quad \cdots \quad Q_{k,p}]^T \in \mathbb{R}^p$. The previous study (which did not consider the scale issue) expressed $Q_{k,j}$ as $Q_{k,j} = |\theta_{k,j}| Q_{0,j}$, where $Q_{0,j}$ is the initial value of

$Q_{k,j}$ [53].

On the other hand, in this study, we propose the novel expression of Q_k by θ_k as

$$Q_k = Q_k(\theta_k) = [10^{\theta_{k,1}} \quad 10^{\theta_{k,2}} \quad \cdots \quad 10^{\theta_{k,p}}]^T \tag{12}$$

Although this transformation is simple, it can effectively reduce the scale differences. For example, suppose that the desired value of Q_k, say Q_k^*, is $Q_k^* = [13.8072 \quad 0.0019]^T$. If the expression in the previous study is employed, then $|\theta_{k,1}|/|\theta_{k,2}|$, the magnitude ratio between $\theta_{k,1}$ and $\theta_{k,2}$, becomes about 7267, where $Q_{0,1} = Q_{0,2} = 1$ [53]. By contrast, if Eq. (12) is used, $|\theta_{k,1}|/|\theta_{k,2}|$ is about 0.4190. Consequently, Eq. (12) can reduce the scale difference in the design variable. This reduced scale difference leads to a design variable that is more suitable to be tuned by SPSA, resulting in improved efficiency of the tuning procedure.

3.4. Tuning algorithm for the VCO-based model-free controller

Figure 3 shows flowchart of the proposed controller tuning scheme for the VCO-based control system. $C_{stop} \in \mathbb{N}$ is the upper bound of the number of iterations. The proposed method shown in Fig. 3 can be conducted iteratively using a computer. Note that neither the actual controlled object models nor the actual mechanical plant itself is required for this procedure. It is because vibration control simulations with the RCO instead of actual object model are used to evaluate the control performance and SPSA only needs the loss function values, which are obtained through simulations with the RCO. The SPSA algorithm automatically searches the controller parameter. Moreover, this tuning algorithm is much faster than the previous algorithm [53] due to the novel parameter transformation shown in Eq. (12). Therefore, the proposed controller tuning procedure significantly improves the practicability of the VCO-base model-free vibration control.

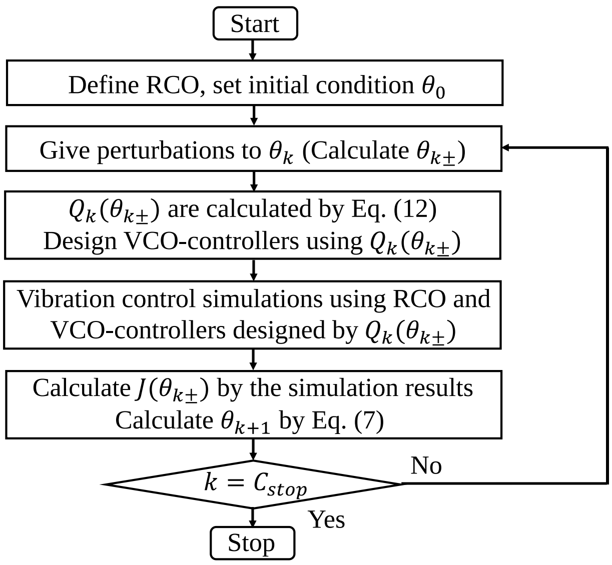

Fig. 3. Flowchart of the proposed controller tuning scheme.

4. Validation of the proposed method via tuning of VCO-based model-free H_2 controller

4.1. Model-free H_2 controller based on VCO

A VCO-based model-free H_2 controller is designed using the 2DOF system shown in Eq. (1). Figure 4 shows the generalized plant for controller design at the kth iteration. The formulations of the 2DOF plant and the controlled variables in Fig. 4 are

$$P_{mf}: \begin{cases} \dot{x}_{mf} = A_{mf}x_{mf} + B_{mf1}w + B_{mf2}u \\ y = C_{mf}x_{mf} + D_{mf1}w + D_{mf2}u \end{cases} \tag{13}$$

$$I: \begin{cases} \dot{x}_I = A_I x_I + B_I y \\ vl = C_I x_I + D_I y \end{cases} \tag{14}$$

$$z = [z_{vl} \quad z_u]^T = [(Q_{k,1})^{0.5}vl \quad (Q_{k,2})^{0.5}u]^T \tag{15}$$

Equation (13) is the state equation of the 2DOF system composed of the actuator and the VCO shown in Eq. (1). y is the acceleration of the VCO. Equation (14) is the realization of the approximate integrator $(s + 1.0 \times 10^{-7})^{-1}$ where s is the Laplace variable. vl is the velocity of the VCO, and $Q_{k,1}$ and $Q_{k,2}$ in Eq. (15) are constant weights to be determined by the proposed method. That is, $Q_k = [Q_{k,1} \quad Q_{k,2}]^T$ is the tuning parameter of this study. w and z are the disturbance and the controlled output, respectively. Accordingly, K_k, the VCO-based model-free H_2 controller at the kth iteration, is designed to minimize $\|\mathcal{F}_l(G_k, K_k)\|_2$, which is the 2-norm of $\mathcal{F}_l(G_k, K_k)$, the closed-loop transfer function from w to z [57]. The Control System Toolbox and the Robust Control Toolbox of MATLAB were used for the numerical calculations.

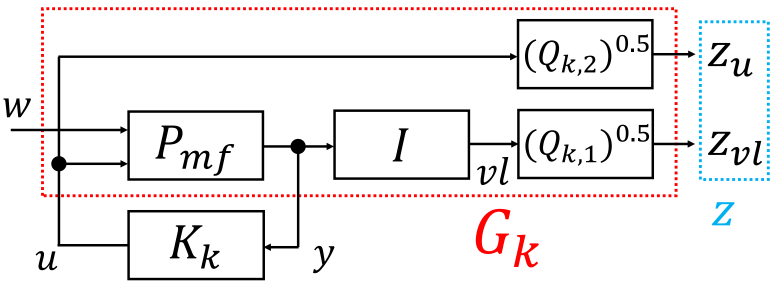

Fig. 4. Generalized plant for VCO-based model-free H_2 controller design.

The effectiveness of the proposed tuning method is verified by tuning Q_k to provide sufficient damping performance for the RCO and actual controlled objects. In particular, the tuning speed of the proposed method is compared with that of the tuning scheme proposed in the previous study [53]. Hereafter, the tuning methods proposed in the previous study and this study are referred to as Algorithms 1 and 2, respectively. Equations (16) and (17) are the expressions of Q_k by θ_k in Algorithms 1 and 2, respectively. Notably, Eq. (16) was used in the previous study [53] and Eq. (17) was proposed in Section 3.3. Table 3 lists the parameters for Algorithms 1 and 2 [53,54]. In the damping simulations, the disturbance to excite the RCO is a white noise.

$$\text{Algorithm 1: } Q_k = Q_0[|\theta_{k,1}| \quad |\theta_{k,2}|]^T \tag{16}$$

$$\text{Algorithm 2: } Q_k = [10^{\theta_{k,1}} \quad 10^{\theta_{k,2}}]^T \tag{17}$$

Table 3. Parameters for Algorithms 1 and 2.

Properties	Value	
	Algorithm 1	Algorithm 2
Δ_k	Bernoulli ±1 distribution with probability of 0.5 for each ±1 outcome	Bernoulli ±1 distribution with probability of 0.5 for each ±1 outcome
a	1.0	3.0
c	3.0×10^{-1}	3.0×10^{-1}
A	1.0×10^{1}	1.0×10^{1}
α	0.602	0.602
γ	0.101	0.101
θ_0	$[1 \quad 1]^T$	$[0 \quad 0]^T$
Q_0	$diag\{1 \quad 1\}$	-
C_{stop}	1500	200

4.2. Tuning results

Figures 5 and 6 are the tuning results obtained by Algorithms 1 and 2, respectively. Figures 5(a) and 6(a) show J_k, the loss function measurement values at each iteration. Figures 5(a) and 6(a) demonstrate that both Algorithms 1 and 2 successfully decrease the measured loss function values as the iterations progress. Notably, Algorithm 2 is much more efficient than Algorithm 1 in that Algorithm 2 can decrease the loss function value with fewer iterations than Algorithm 1. Figures 5(b) and 6(b) describe the frequency responses obtained by the vibration control simulation for the RCO. In Fig. 5(b), the black, blue, and red lines indicate the frequency response without control, the closed-loop frequency response with the controller designed by Q_0, and the closed-loop frequency response with the controller designed by Q_{1500}, respectively. In Fig. 6(b), the black, blue, and green lines show the frequency response without control, the closed-loop frequency response with control by Q_0, and the closed-loop frequency response with control by Q_{200}, respectively. That is, the blue lines in Figs. 5(b) and 6(b) are the frequency responses provided by the controller before tuning, whereas the red and green lines are those provided by the controller after tuning via Algorithms 1 and 2, respectively. The black and blue lines almost overlap in Figs. 5(b) and 6(b). Table 4 lists the Q_k and J_k values obtained by Algorithms 1 and 2, respectively. Figures 5 and 6 demonstrate that both Algorithms 1 and 2 can determine the proper tuning parameters and that the resultant controllers provide good damping performance for the RCO. The resultant controllers have the same damping performance for the RCO. However, Figs. 5 and 6 and Table 4 also show that Algorithm 2 can search the appropriate tuning parameter much faster than the previous method. Consequently, Algorithm 2 is more efficient than Algorithm 1.

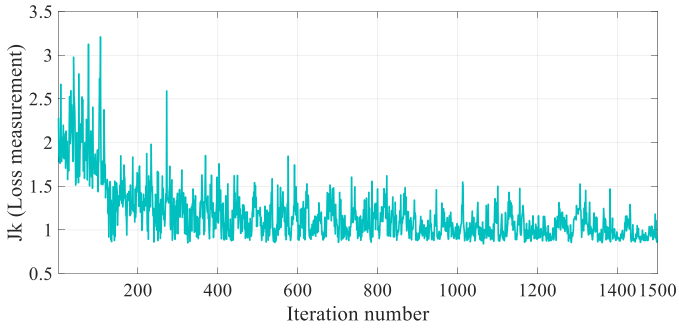

(a)

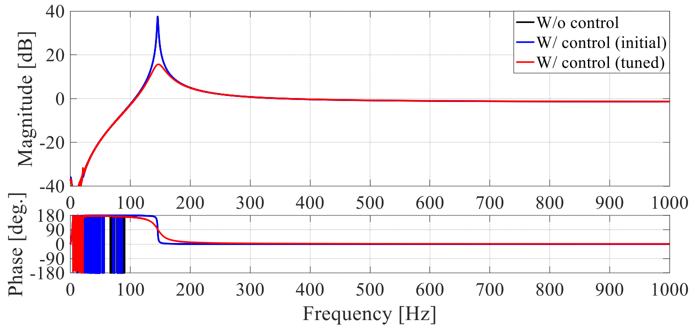

(b)

Fig. 5. Results of tuning by Algorithm 1: (a) J_k, and (b) frequency responses obtained by the vibration control simulations for the RCO.

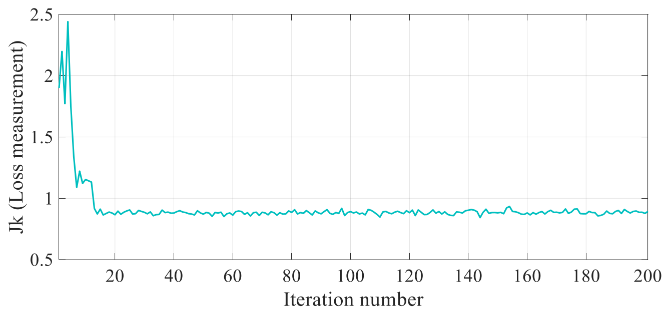

(a)

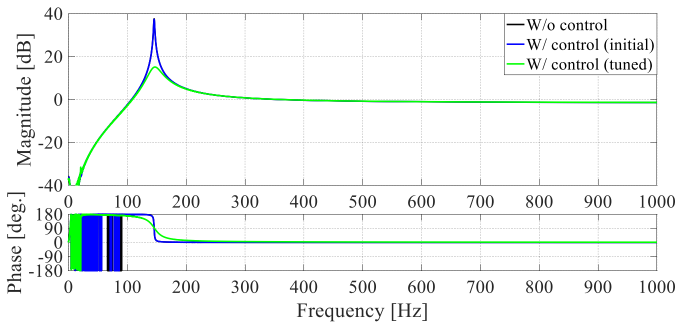

(b)

Fig. 6. Results of tuning by Algorithm 2: (a) J_k, and (b) frequency responses obtained by the vibration control simulations for the RCO.

Additionally, we performed the same validation as described in Section 4.1 when values of m_v and k_v are fluctuated by $\pm 30\%$ each. The other conditions for the tuning are the same as those for the validation shown in Figs. 5 and 6. As a result, almost the same results as those demonstrated in Figs. 5 and 6 have been obtained. That is, although both Algorithms 1 and 2 provided the appropriate parameters of the VCO-based H_2 controller, Algorithm 2 outperformed Algorithm 1 in the viewpoint of the tuning speed. Therefore, the proposed method has robustness to parameter variations of the VCO.

Table 4. Tuning results.

Properties	Value	
	Algorithm 1	Algorithm 2
$Q_{Cstop,1}$	3.0283	1.2651×10^2
$Q_{Cstop,2}$	3.5194×10^{-4}	0.0108
J_0	2.2823	1.9001
J_{Cstop}	0.9112	0.8927

5. Vibration control experiment

The damping performance of the VCO-based model-free H_2 controller tuned by the proposed method (Algorithm 2) is compared with that of the controller tuned by the previous method (Algorithm 1) via vibration control experiments. Hereafter, the controller tuned by Algorithm 1 is referred to as Controller 1 and that tuned by Algorithm 2 is referred to as Controller 2. Controllers 1 and 2 were designed using the parameters listed in Table 4. Notably, Controllers 1 and 2 are identical to the controllers which provide the control results described by the red line in Fig. 5(b) and the green line in Fig. 6(b), respectively.

Figure 7 shows the experimental setup and the closed-loop system configuration. The damping performance of the controllers is evaluated by the acceleration of the controlled object. In the experimental system, the actuator was fixed on the damping point of the actual controlled object with bolts and nuts; the acceleration sensor was fixed with a magnet. The sensor was attached on the backside of the position where the actuator was mounted. The measured output was obtained by the accelerometer and input to the digital signal processor (DSP). The DSP calculated the control input signal on the basis of the measured output. The control input signal provided by the DSP passed through an analog low-pass filter to prevent spillover. The control signal was then amplified by the current amplifier to drive the actuator. The disturbance (a 1–1000 Hz linear sweep sinusoidal signal) was delivered from the signal generator. The spectrum analyzer measured the frequency responses from the disturbance to the acceleration of the damping point. Figure 8 describes the controlled objects for the experiments. The structure shown in Fig. 8(a) is a cantilever plate made of aluminum, and the structure shown in Fig. 8(b) is the cantilever plate (described in Fig. 8(a)) with a 0.685 kg mass on it. Hereafter, the structures depicted in Fig. 8(a) and 8(b) are referred to as Controlled Objects 1 and 2, respectively.

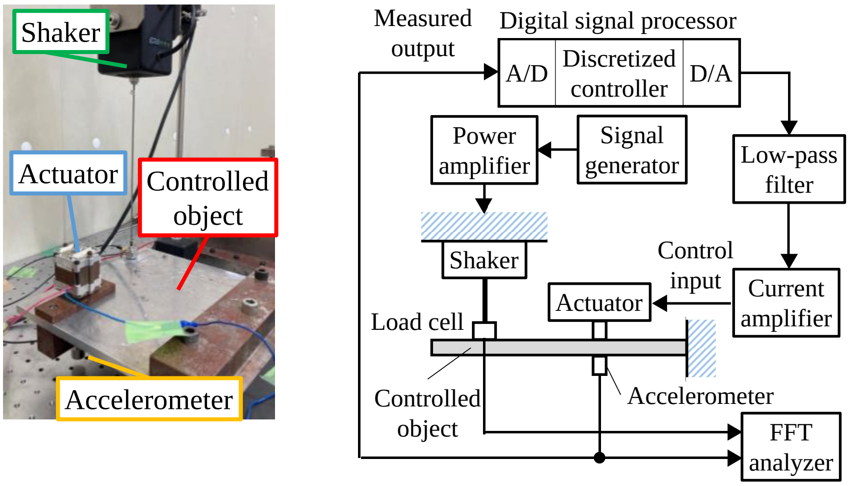

(a) (b)

Fig. 7. Experimental system: (a) experimental setup, and (b) closed-loop configuration.

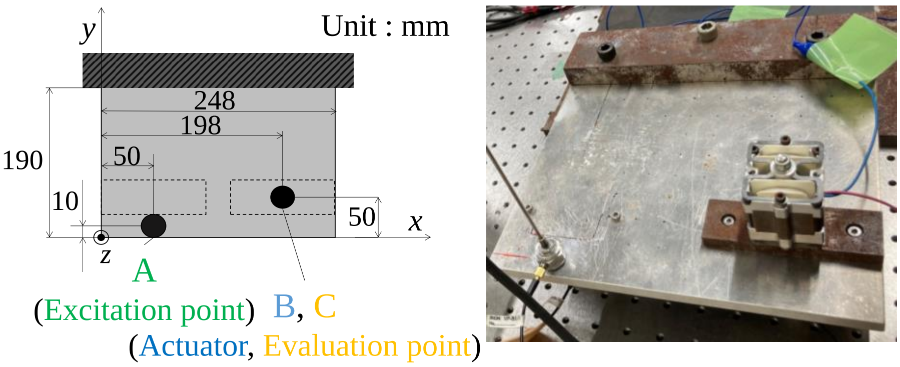

(a)

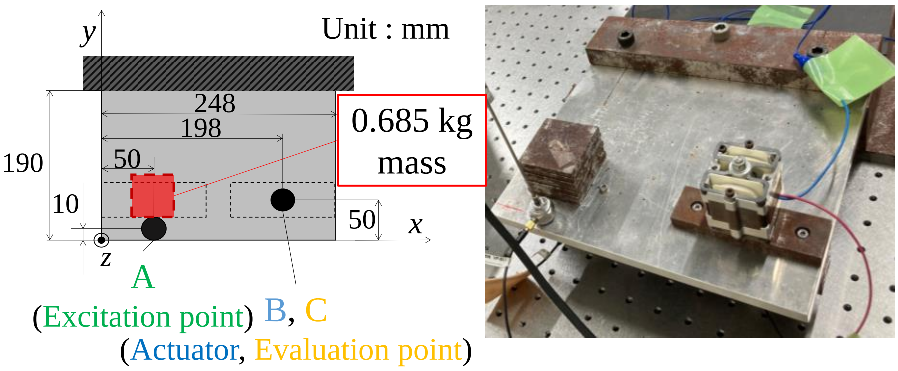

(b)

Fig. 8. Configurations of controlled objects: (a) Controlled Object 1 (cantilever plate), and (b) Controlled Object 2 (Controlled Object 1 with a 0.685 kg mass on it).

Figures 9 and 10 show the experimental results for Controlled Objects 1 and 2, respectively. The black, red, and green lines are the frequency response without control, the closed-loop frequency response with Controller 1, and the closed-loop frequency response with Controller 2, respectively. Table 5 summarizes the representative damping results in Figs. 9 and 10. The results in Figs. 9 and 10 and Table 5 show that both Controllers 1 and 2 provided good damping effects to Controlled Objects 1 and 2. The vibration suppression performance of Controller 2 is the same as that of Controller 1. Notably, however, Controller 2 is obtained using a much smaller number of iterations than Controller 1. That is, Algorithm 2 is much more efficient than Algorithm 1 because Algorithm 2 can provide an appropriate tuning parameter of the VCO-based model-free controller with a much smaller number of iterations than Algorithm 1.

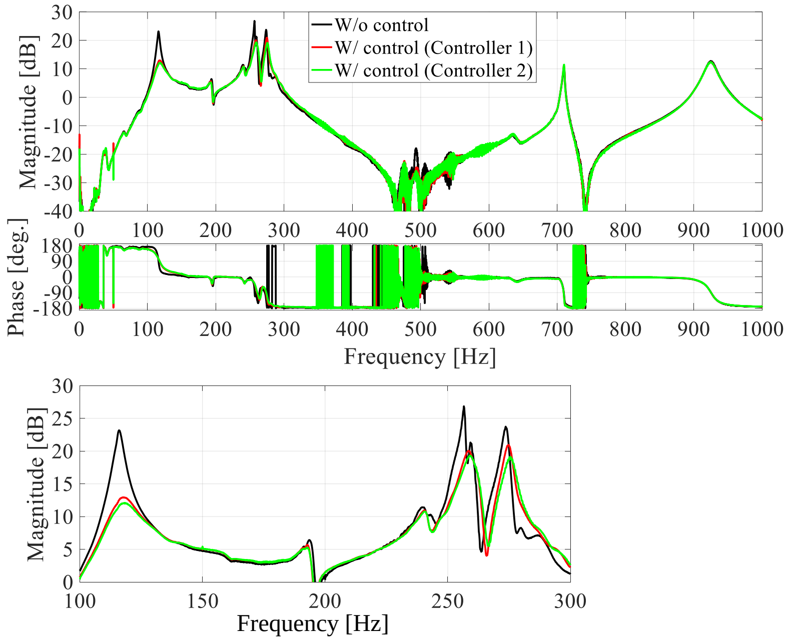

Fig. 9. Frequency responses obtained by vibration control experiments with Controlled Object 1.

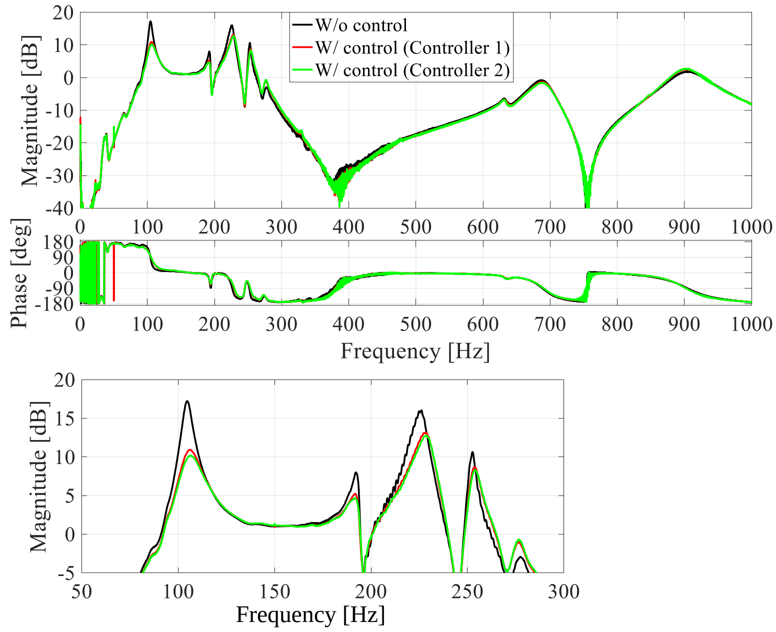

Fig. 10. Frequency responses obtained by vibration control experiments with Controlled Object 2.

Table 5. Main vibration reductions for Controlled Objects 1 and 2.

Controller	Reduction amount [dB]			
	Controlled Object 1		Controlled Object 2	
	116 Hz peak	257 Hz peak	105 Hz peak	226 Hz peak
Controller 1	-10.23	-6.79	-6.28	-2.87
Controller 2	-11.11	-7.52	-7.01	-3.21

6. Discussion

Section 4.2 shows that the proposed method appropriately tunes the VCO-based model-free H_2 controller to provide good damping effects to the RCO without burdensome manual trial-and-errors. In Chapter 5, we demonstrated that the controller tuned by the proposed algorithm can suppress the vibrations occurring at various controlled objects that differ from the RCO. Therefore, the proposed method can derive a VCO-controller that is applicable to various structures without requiring modeling and trial-and-error tunings for them.

Although Controllers 1 and 2 are tuned using only the RCO, they both suppress vibrations occurring not only at the RCO but also at various controlled objects other than the RCO, as shown in Chapter 5. These results are attributed to the VCO-based model-free controller being robust against various changes in actual controlled objects [53]. Such robustness is due to the independence of the VCO-based controller design from actual controlled objects. Moreover, Controllers 1 and 2 are tuned using different methods—specifically, Algorithms 1 and 2—implying that such robustness does not depend on the parameter tuning procedure. Therefore, more appropriate scaling methods and parameter searching algorithms might exist. In the future, several types of scaling and optimization techniques will be compared.

The significant difference between Algorithms 1 and 2 is the tuning parameter expression, i.e., only Algorithm 2 addresses the scale difference in the tuning parameters. The tuning results shown in Table 4 confirm that the resultant tuning parameters differ substantially in scale. Specifically, in Algorithm 1, $Q_{Cstop,1}/Q_{Cstop,2} \approx 8.6 \times 10^3$, and $Q_{Cstop,1}/Q_{Cstop,2} \approx 1.2 \times 10^4$ in Algorithm 2. However, the scale difference in the design variables in Algorithm 2 is much smaller than that in Algorithm 1: $|\theta_{Cstop,1}|/|\theta_{Cstop,2}| \approx 8.6 \times 10^3$ in Algorithm 1, and $|\theta_{Cstop,1}|/|\theta_{Cstop,2}| \approx 1.1$ in Algorithm 2. These differences originate from Eq. (12), which appropriately modifies the design variables to fit SPSA. Consequently, the proposed parameter expression greatly reduces the scale differences of the parameters to be tuned and improves the speed of the tuning algorithm, resulting in enhancing the practicability of the VCO-based model-free vibration control.

The VCO-based active damping method is simple and practical in the sense that this method does not require any mathematical models of actual controlled objects for its design process. This damping technique can be used by directly attaching the actuator and sensor to the damping point. Nevertheless, this condition may not always be satisfied depending on size of the actuator, configuration of the structure to be controlled, and so on. In the future, to further improve the practicability, the VCO-based model-free vibration control method will be modified so as to be feasible even if the actuator and the sensor cannot be attached directly to the damping point.

This study treats rather a practical issue of the VCO-method than exploring its fundamental characteristics so as to bridge the gap between the basic study and its implementation. In particular, this study is devoted to reducing the labor of tuning of the VCO-based model-free controller, enhancing the implementation of the VCO-based model-free vibration control in practice. However, the several fundamental natures of the VCO-based model-free control system such as the stability have not been rigorously analyzed so far. The analysis of the VCO-method may require different techniques from the way to analyze usual model-based control systems due to its model-free nature. In the future, the analysis method of the model-free control system based on the VCO will be developed, and the stability of the VCO-based model-free control will be theoretically analyzed.

As demonstrated in the experiments, the VCO-based model-free vibration control technique can suppress multiple modes vibration in the predetermined frequency band where vibration should be attenuated, which is a significant advantage of this control strategy. This is because VCO-based model-free control relies on the condition that $x_v \approx x_1$ holds in the controlled frequency band. Specifically, VCO-based control indirectly suppresses the vibration x_1 of the actual controlled object via controlling x_v of the VCO. This implies that every mode vibration making magnitude of x_1 (and hence x_v) large in the controlled frequency band is attenuated by the VCO-based model-free controller. Consequently, if there exist multiple vibrations having large magnitude within the controlled frequency band, VCO-based model-free control can suppress the vibration due to all of them, resulting in multi-mode vibration control. Note that the condition $x_v \approx x_1$, which is the key for VCO-based model-free vibration control, can be achieved independently of detailed vibration characteristics of the actual controlled object.

However, the mechanism of VCO-based model-free vibration control also implies its limitation: this technique is not good at reducing the vibrations having small magnitudes at the damping point. For example, vibration due to a mode where the damping point locates nearly at its node cannot be suppressed. That is, although the VCO-based model-free vibration control technique is effective for suppressing distinguished vibration modes at the damping point, other vibration modes tend to be neglected. Employing multiple actuators will be effective to overcome this difficulty and to achieve good vibration suppression at multiple damping points; this will be our future work.

7. Conclusion

In this article, a novel controller tuning method is developed to enhance the practicability of the VCO-based model-free vibration control. The proposed tuning strategy was compared with the previous one via tuning the VCO-based model-free H_2 controller, exhibiting the better performance. In the experimental verifications, the controller tuned by the proposed method provided good damping effects for all the investigated controlled objects. Consequently, this study successfully improves the usability of the VCO-based model-free vibration control, resulting in providing the simple and practical technique to tackle the vibration problems for various mechanical systems.

In the future, the performance of the proposed method will be verified for tuning problems of VCO-based model-free controllers designed using various types of control strategies because the proposed method does not depend on specific types of the control theory to design a VCO-controller. Moreover, the VCO-based model-free active damping method will be modified so that it can be used when the actuator and the sensor cannot be attached directly to the damping point.

CRediT authorship contribution statement

Ansei Yonezawa: Conceptualization, Methodology, Software, Validation, Investigation, Writing - Original Draft. **Heisei Yonezawa**: Methodology, Software, Validation. **Itsuro Kajiwara**: Conceptualization, Writing - Original Draft, Supervision.

Acknowledgements

We thank the Japan Society for the Promotion of Science (JSPS) for their support (Grant no. JP22J11365).

References

[1] G. Jiang, X. Jing, Y. Guo, A novel bio-inspired multi-joint anti-vibration structure and its nonlinear HSLDS properties, Mech. Syst. Signal Process. 138 (2020) 106552. https://doi.org/10.1016/j.ymssp.2019.106552.

[2] Z. Zhang, J. Zhang, H. Yin, B. Zhang, X. Jing, Bio-inspired structure reference model oriented robust full vehicle active suspension system control via constraint-following, Mech. Syst. Signal Process. 179 (2022) 109368. https://doi.org/10.1016/j.ymssp.2022.109368.

[3] Y. Wang, X. Jing, Nonlinear stiffness and dynamical response characteristics of an asymmetric X-shaped structure, Mech. Syst. Signal Process. 125 (2019) 142–169. https://doi.org/10.1016/j.ymssp.2018.03.045.

[4] X. Feng, X. Jing, Z. Xu, Y. Guo, Bio-inspired anti-vibration with nonlinear inertia coupling, Mech. Syst. Signal Process. 124 (2019) 562–595. https://doi.org/10.1016/j.ymssp.2019.02.001.

[5] K. Ye, J.C. Ji, An origami inspired quasi-zero stiffness vibration isolator using a novel truss-spring based stack Miura-ori structure, Mech. Syst. Signal Process. 165 (2022) 108383. https://doi.org/10.1016/j.ymssp.2021.108383.

[6] J.C. Ji, Q. Luo, K. Ye, Vibration control based metamaterials and origami structures: A state-of-the-art review, Mech. Syst. Signal Process. 161 (2021) 107945. https://doi.org/10.1016/j.ymssp.2021.107945.

[7] H. Yonezawa, I. Kajiwara, S. Sato, C. Nishidome, M. Sakata, T. Hatano, S. Hiramatsu, Vibration control of automotive drive system with nonlinear gear backlash, J. Dyn. Syst. Meas. Control. Trans. ASME. 141 (2019) 121002. https://doi.org/10.1115/1.4044614.

[8] H. Yonezawa, A. Yonezawa, T. Hatano, S. Hiramatsu, C. Nishidome, I. Kajiwara, Fuzzy-reasoning-based robust vibration controller for drivetrain mechanism with various control input updating timings, Mech. Mach. Theory. 175 (2022) 104957. https://doi.org/10.1016/j.mechmachtheory.2022.104957.

[9] H. Yonezawa, I. Kajiwara, C. Nishidome, T. Hatano, M. Sakata, S. Hiramatsu, Active vibration control of automobile drivetrain with backlash considering time-varying long control period, Proc. Inst. Mech. Eng. Part D J. Automob. Eng. 235 (2021) 773–783. https://doi.org/10.1177/0954407020949428.

[10] X. Wei, J.E. Mottershead, Block-decoupling vibration control using eigenstructure assignment, Mech. Syst. Signal Process. 74 (2016) 11–28. https://doi.org/10.1016/j.ymssp.2015.03.028.

[11] X. Wei, R. Xia, J.E. Mottershead, X. He, <math altimg="si1.svg"> <mrow> <msub> <mi mathvariant="script">H</mi> <mn>2</mn> </msub> </mrow> </math> -optimal vibration control using receptance-based regional eigenvalue assignment, Mech. Syst. Signal Process. 167 (2022) 108591. https://doi.org/10.1016/j.ymssp.2021.108591.

[12] T. Atsumi, S. Yabui, Quadruple-Stage Actuator System for Magnetic-Head Positioning System in Hard Disk Drives, IEEE Trans. Ind. Electron. 67 (2020) 9184–9194. https://doi.org/10.1109/TIE.2019.2955432.

[13] S. Yabui, T. Atsumi, T. Inoue, Coupling Controller Design for MISO System of Head Positioning Control Systems in HDDs, IEEE Trans. Magn. 56 (2020). https://doi.org/10.1109/TMAG.2020.2978156.

[14] S. Yabui, T. Atsumi, T. Inoue, Servo Controller Design for Triple-Stage Actuator in HDD to Compensate for High-Frequency Fan Vibration, IEEE Trans. Magn. 58 (2022). https://doi.org/10.1109/TMAG.2021.3129540.

[15] A. Concha, S. Thenozhi, R.J. Betancourt, S.K. Gadi, A tuning algorithm for a sliding mode controller of buildings with ATMD, Mech. Syst. Signal Process. 154 (2021) 107539. https://doi.org/10.1016/j.ymssp.2020.107539.

[16] S. Wan, X. Li, W. Su, J. Yuan, J. Hong, Active chatter suppression for milling process with sliding mode control and electromagnetic actuator, Mech. Syst. Signal Process. 136 (2020) 106528. https://doi.org/10.1016/j.ymssp.2019.106528.

[17] P. Zech, D.F. Plöger, S. Rinderknecht, Active control of planetary gearbox vibration using phase-exact and narrowband simultaneous equations adaptation without explicitly identified secondary path models, Mech. Syst. Signal Process. 120 (2019) 234–251. https://doi.org/10.1016/j.ymssp.2018.10.030.

[18] Y. Yu, Z. Yang, C. Han, H. Liu, Active Vibration Control of Magnetically Suspended Wheel Using Active Shaft Deflection, IEEE Trans. Ind. Electron. 64 (2017) 6528–6537. https://doi.org/10.1109/TIE.2017.2682786.

[19] T. Chen, J. Lou, Y. Yang, Z. Ren, C. Xu, Vibration Suppression of a High-Speed Macro-Micro Integrated System Using Computational Optimal Control, IEEE Trans. Ind. Electron. 67 (2020) 7841–7850. https://doi.org/10.1109/TIE.2019.2941136.

[20] M. Zhang, X. Jing, Model-free saturated PD-SMC method for 4-DOF tower crane systems, IEEE Trans. Ind. Electron. 69 (2022) 10270–10280. https://doi.org/10.1109/TIE.2021.3139134.

[21] M. Zhang, X. Jing, A Bioinspired Dynamics-Based Adaptive Fuzzy SMC Method for Half-Car Active Suspension Systems with Input Dead Zones and Saturations, IEEE Trans. Cybern. 51 (2021) 1743–1755. https://doi.org/10.1109/TCYB.2020.2972322.

[22] Y. Mousavi, A. Alfi, I.B. Kucukdemiral, A. Fekih, Tube-based Model Reference Adaptive Control for Vibration Suppression of Active Suspension Systems, IEEE/CAA J. Autom. Sin. 9 (2022) 728–731. https://doi.org/10.1109/JAS.2022.105470.

[23] O. Abdeljaber, O. Avci, D.J. Inman, Active vibration control of flexible cantilever plates using piezoelectric materials and artificial neural networks, J. Sound Vib. 363 (2016) 33–53. https://doi.org/10.1016/j.jsv.2015.10.029.

[24] W. He, Y. Ouyang, J. Hong, Vibration Control of a Flexible Robotic Manipulator in the Presence of Input Deadzone, IEEE Trans. Ind. Informatics. 13 (2017) 48–59. https://doi.org/10.1109/TII.2016.2608739.

[25] M. Zhang, X. Jing, G. Wang, Bioinspired Nonlinear Dynamics-Based Adaptive Neural Network Control for Vehicle Suspension Systems with Uncertain/Unknown Dynamics and Input Delay, IEEE Trans. Ind. Electron. 68 (2021) 12646–12656. https://doi.org/10.1109/TIE.2020.3040667.

[26] H. Ma, H. Ren, Q. Zhou, R. Lu, H. Li, Approximation-Based Nussbaum Gain Adaptive Control of Nonlinear Systems with Periodic Disturbances, IEEE Trans. Syst. Man, Cybern. Syst. 52 (2022) 2591–2600. https://doi.org/10.1109/TSMC.2021.3050993.

[27] B. Li, X. Rui, Vibration control of uncertain multiple launch rocket system using radial basis function neural network, Mech. Syst. Signal Process. 98 (2018) 702–721. https://doi.org/10.1016/j.ymssp.2017.05.036.

[28] K. Szabat, T. Tran-Van, M. Kaminski, A Modified Fuzzy Luenberger Observer for a Two-Mass Drive System, IEEE Trans. Ind. Informatics. 11 (2015) 531–539. https://doi.org/10.1109/TII.2014.2327912.

[29] H.-L. Bui, C.-H. Nguyen, V.-B. Bui, K.-N. Le, H.-Q. Tran, Vibration control of uncertain structures with actuator saturation using hedge-algebras-based fuzzy controller, J. Vib. Control. 23 (2017) 1984–2002. https://doi.org/10.1177/1077546315606601.

[30] Y. Fang, J. Fei, T. Hu, Adaptive backstepping fuzzy sliding mode vibration control of flexible structure, J. Low Freq. Noise Vib. Act. Control. 37 (2018) 1079–1096. https://doi.org/10.1177/1461348418767097.

[31] O. Kaneko, S. Souma, T. Fujii, Fictitious Reference Iterative Tuning in the Two-Degree of Freedom Control Scheme and Its Application to a Facile Closed Loop System Identification, Trans. Soc. Instrum. Control Eng. 42 (2006) 17–25.

[32] C.L. Remes, R.B. Gomes, J.V. Flores, F.B. Libano, L. Campestrini, Virtual Reference Feedback Tuning Applied to DC-DC Converters, IEEE Trans. Ind. Electron. 68 (2021) 544–552. https://doi.org/10.1109/TIE.2020.2967729.

[33] J. Han, From PID to active disturbance rejection control, IEEE Trans. Ind. Electron. 56 (2009) 900–906. https://doi.org/10.1109/TIE.2008.2011621.

[34] S. Zhao, Z. Gao, An active disturbance rejection based approach to vibration suppression in two-inertia systems, Asian J. Control. 15 (2013) 350–362. https://doi.org/10.1002/asjc.552.

[35] Q. Zheng, H. Richter, Z. Gao, Active disturbance rejection control for piezoelectric beam, Asian J. Control. 16 (2014) 1612–1622. https://doi.org/10.1002/asjc.854.

[36] S. Li, C. Zhu, Q. Mao, J. Su, J. Li, Active disturbance rejection vibration control for an all-clamped piezoelectric plate with delay, Control Eng. Pract. 108 (2021) 104719. https://doi.org/10.1016/j.conengprac.2020.104719.

[37] H. Yonezawa, I. Kajiwara, A. Yonezawa, Experimental verification of model-free active vibration control approach using virtually controlled object, J. Vib. Control. 26 (2020) 1656–1667. https://doi.org/10.1177/1077546320902348.

[38] A. Yonezawa, H. Yonezawa, I. Kajiwara, Vibration control for various structures with time-varying properties via model-free adaptive controller based on virtual controlled object and SPSA, Mech. Syst. Signal Process. 170 (2022) 108801. https://doi.org/10.1016/j.ymssp.2022.108801.

[39] A. Yonezawa, I. Kajiwara, H. Yonezawa, Model-free vibration control based on a virtual controlled object considering actuator uncertainty, J. Vib. Control. 27 (2021) 1324–1335. https://doi.org/10.1177/1077546320940922.

[40] A. Yonezawa, I. Kajiwara, H. Yonezawa, Novel Sliding Mode Vibration Controller With Simple Model-Free Design and Compensation for Actuator's Uncertainty, IEEE Access. 9 (2021) 4351–4363. https://doi.org/10.1109/ACCESS.2020.3047810.

[41] A. Yonezawa, H. Yonezawa, I. Kajiwara, Experimental study of model-free vibration control based on a virtual controlled object considering parameter uncertainty of actuator, Proc. Inst. Mech. Eng. Part C J. Mech. Eng. Sci. in press (2022) 1–10. https://doi.org/10.1177/09544062221140814.

[42] L. Li, L. Xie, X. Luo, Z. Wang, Compliance Control Using Hydraulic Heavy-Duty Manipulator, IEEE Trans. Ind. Informatics. 15 (2019) 1193–1201. https://doi.org/10.1109/TII.2018.2873256.

[43] P. Mandal, B.K. Sarkar, R. Saha, S. Mookherjee, S.K. Acharyya, D. Sanyal, GA-Optimized Fuzzy-Feedforward-Bias Control of Motion by a Rugged Electrohydraulic System, IEEE/ASME Trans. Mechatronics. 20 (2015) 1734–1742. https://doi.org/10.1109/TMECH.2014.2352156.

[44] R. Patel, F. Hafiz, A. Swain, A. Ukil, Nonlinear Excitation Control of Diesel Generator: A Command Filter Backstepping Approach, IEEE Trans. Ind. Informatics. 17 (2021) 4809–4817. https://doi.org/10.1109/TII.2020.3017744.

[45] R.-E. Precup, R.-C. David, E.M. Petriu, M.-B. Rădac, S. Preitl, Adaptive GSA-based optimal tuning of PI controlled servo systems with reduced process parametric

sensitivity, robust stability and controller robustness, IEEE Trans. Cybern. 44 (2014) 1997–2009. https://doi.org/10.1109/TCYB.2014.2307257.

[46] R.-E. Precup, R.-C. David, E.M. Petriu, Grey Wolf Optimizer Algorithm-Based Tuning of Fuzzy Control Systems With Reduced Parametric Sensitivity, IEEE Trans. Ind. Electron. 64 (2017) 527–534. https://doi.org/10.1109/TIE.2016.2607698.

[47] R.C. Roman, R.-E. Precup, C.A. Bojan-Dragos, A.I. Szedlak-Stinean, Combined Model-Free Adaptive Control with Fuzzy Component by Virtual Reference Feedback Tuning for Tower Crane Systems, Procedia Comput. Sci. 162 (2019) 267–274. https://doi.org/10.1016/j.procs.2019.11.284.

[48] R.-C. Roman, R.-E. Precup, E.M. Petriu, Hybrid data-driven fuzzy active disturbance rejection control for tower crane systems, Eur. J. Control. 58 (2021) 373–387. https://doi.org/10.1016/j.ejcon.2020.08.001.

[49] E.D.P. Puchta, H.V. Siqueira, M.D.S. Kaster, Optimization Tools Based on Metaheuristics for Performance Enhancement in a Gaussian Adaptive PID Controller, IEEE Trans. Cybern. 50 (2020) 1185–1194. https://doi.org/10.1109/TCYB.2019.2895319.

[50] J.C. Spall, Multivariate Stochastic Approximation Using a Simultaneous Perturbation Gradient Approximation, IEEE Trans. Automat. Contr. 37 (1992) 332–341. https://doi.org/10.1109/9.119632.

[51] M.-B. Rădac, R.-E. Precup, E.M. Petriu, S. Preitl, Application of IFT and SPSA to servo system control, IEEE Trans. Neural Networks. 22 (2011) 2363–2375. https://doi.org/10.1109/TNN.2011.2173804.

[52] M.A. Ahmad, S.I. Azuma, T. Sugie, Performance analysis of model-free PID tuning of MIMO systems based on simultaneous perturbation stochastic approximation, Expert Syst. Appl. 41 (2014) 6361–6370. https://doi.org/10.1016/j.eswa.2014.03.055.

[53] A. Yonezawa, H. Yonezawa, I. Kajiwara, Parameter tuning technique for a model-free vibration control system based on a virtual controlled object, Mech. Syst. Signal Process. 165 (2022) 108313. https://doi.org/10.1016/j.ymssp.2021.108313.

[54] J.C. Spall, Implementation of the simultaneous perturbation algorithm for stochastic optimization, IEEE Trans. Aerosp. Electron. Syst. 34 (1998) 817–823. https://doi.org/10.1109/7.705889.

[55] R. Madonski, P. Herman, Model-Free Control or Active Disturbance Rejection Control? on different approaches for attenuating the perturbation, in: 2012 20th Mediterr. Conf. Control Autom. MED 2012 - Conf. Proc., IEEE, 2012: pp. 60–65. https://doi.org/10.1109/MED.2012.6265615.

[56] J.C. Spall, Introduction to Stochastic Search and Optimization, Wiley, Hoboken, New Jersey, 2003.

[57] K. Zhou, J.C. Doyle, K. Glover, Robust and Optimal Control, Prentice Hall, Upper Saddle River, New Jersey, 1996.